

## Phase dynamics near a parity-breaking instability

Laurent Fourtune, Wouter-Jan Rappel, and Marc Rabaud

*Laboratoire de Physique Statistique de L'Ecole Normale Supérieure, 24 rue Lhomond, 75231 Paris Cedex 05, France*

(Received 14 February 1994)

In a directional viscous fingering experiment, a phase diffusion behavior of the regular array of cells is demonstrated. At constant wave number, the evolution of the phase diffusion coefficient  $D$  with the parameter of the instability  $\epsilon$  is reported. This coefficient  $D$  is found to decrease at low  $\epsilon$  values in agreement with the presence of an Eckhaus instability, but to increase strongly at large  $\epsilon$  values. This unusual increase of  $D$  is also present in the analytical and numerical study of two coupled amplitude equations for the modes  $k$  and  $2k$ . The phase diffusion coefficient is found to diverge at the threshold of the parity-breaking bifurcation.

PACS number(s): 47.20.Hw, 47.35.+i, 47.20.Ky

The idea of describing the dynamics of patterns exhibited by forced dissipative systems through a phase equation appeared some years ago [1]. The homogeneity of wave numbers often encountered above an instability threshold has been ascribed to the existence of a diffusive behavior for the phase. Such a diffusive behavior has been found in Rayleigh-Bénard convection [2] and more recently in Taylor vortex flow (TVF) [3]. Just above the threshold, the patterns can be unstable to long wavelength modulations if the phase diffusion constant becomes negative. This instability is known as the Eckhaus instability [4] and limits the range of possible wave numbers for the stable pattern. More recently, it has been shown in numerical simulations of the nonlinear equations of directional growth [5] and TVF [6] that the Eckhaus stable band shrinks due to the nonlinear interactions between the fundamental (mode  $k$ ) and the first harmonic (mode  $2k$ ) of the pattern. Such interactions were first analyzed by Jones and Proctor [7], and it has been shown [8] that these interactions can explain the broken parity propagative state observed in many experimental situations [9]. In this paper we present the phase diffusion dynamics of the interface of a directional viscous fingering (DVF) experiment, and show that for a fixed wave number the phase diffusion constant  $D$  decreases to small values for a decreasing control parameter, but increases to very high values for an increasing control parameter. Both these limits,  $D \rightarrow 0$  and  $D \rightarrow \infty$ , constrain the domain of stable homogeneous stationary patterns. The first behavior is interpreted as a classical Eckhaus instability, but the second is ascribed to the proximity of a parity-breaking bifurcation. This assessment is supported by the analytical study and simulations of two coupled amplitude equations for the  $k$  and  $2k$  modes.

The experimental setup is similar to the one presented in Ref. [10]. Here, one horizontal Plexiglas cylinder is partially immersed in an oil tank. By rotating the cylinder, a coating oil film is dragged out of the tank and fills the small gap between the cylinder and an upper horizontal glass plate [Fig. 1(a)]. For a large enough rotation rate, the downstream meniscus between the cylinder and the glass plate undergoes a supercritical bifurcation, and, seen from above, a periodic deformation of this meniscus appears [Fig. 1(b)]. Here, in contrast to previous studies of DVF, we impose the length  $L$  of the interface by placing two Mylar triangles that fill the gap. Each of these boundaries imposes the position of the last cell [Fig. 1(b)], which is enlarged compared to the other cells.

In Ref. [10] the experimental evolution of the wave number of the instability for increasing and decreasing velocity was reported. Without the Mylar triangles a very strong selection of the wave number exists and no hysteresis was detected. In the present experiment we repeat this study with rigid boundaries. In Fig. 2 we plot the evolution of the wave number  $k$  for increasing and decreasing dimensionless velocity  $\epsilon = \frac{V-V_c}{V_c}$ , where  $V_c = 159$  mm/s is the instability threshold for large  $L$ . The evolution of  $k$  is discontinuous and strongly hysteretic, even for a large number of air cells [11]. Any mode  $k$  is stable if  $\epsilon$  ranges between  $\epsilon_{min}(k)$  and  $\epsilon_{max}(k)$ . We repeated the measurement at  $k = 0.823$  mm<sup>-1</sup> for two lengths  $L$  corresponding to 5 and 22 cells, and the two limits  $\epsilon_{min}(k)$  and  $\epsilon_{max}(k)$  were almost unchanged, showing that small box corrections are negligible.

In order to investigate the nature of the two stability

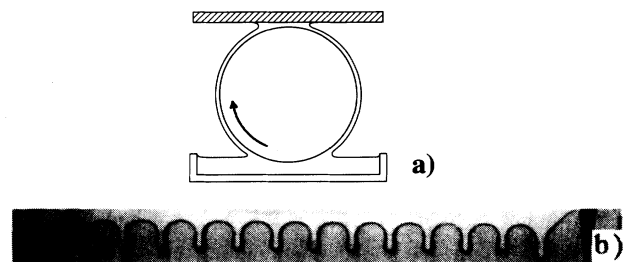


FIG. 1. (a) Sketch of the experimental setup. The rotating cylinder (radius 48 mm and length 236 mm) is partially immersed in a silicon oil bath (viscosity of  $\nu = 20$  mm<sup>2</sup>/s at 25 °C), thermostated at  $25 \pm 0.1$  °C. The coating film fills the small gap ( $b = 0.22 \pm 0.02$  mm) between the upper glass plate and the cylinder, (b) picture of the unstable meniscus, constrained by two Mylar triangles located inside the gap with a spacing of  $L = 57$  mm (dimensionless cylinder velocity  $\epsilon = 1.72$ ).

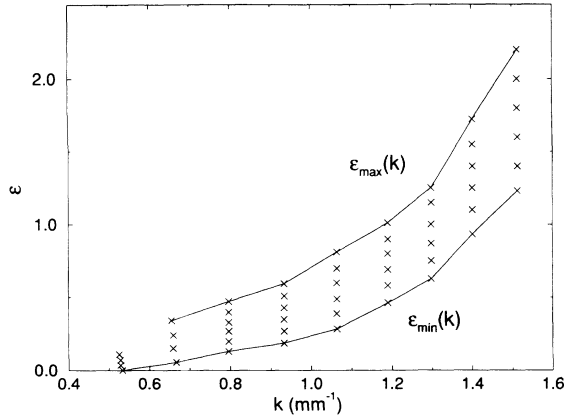


FIG. 2. Experimental data points indicating the domain of existence of stable stationary patterns observed when  $\epsilon$  evolves ( $L = 57$  mm). The number of cells evolves from 4 to 12. The solid lines are guides to the eye.

limits in the plane of Fig. 2, we measured the phase diffusion constant of the pattern as in Ref. [3]. For this purpose, one of the Mylar triangles is forced to oscillate slowly at the frequency  $f$  and the amplitude  $Z_0$ . In Fig. 3 we plot the temporal evolution of one video line crossing all the cells. We see that each oil wall (labeled  $0, 1, \dots, n, \dots$ ) between two air cells oscillates at the forcing frequency. For each wall  $n$ , we measured the amplitude and the phase of this oscillation. We found, to a very good approximation, that the amplitude is proportional to  $e^{-\alpha n \lambda}$ , and that the phase change is equal to  $-\beta n \lambda$ , where  $\lambda$  is the wavelength of the pattern.

For given  $\epsilon$  and  $k$ , we measured  $\alpha$  and  $\beta$  over a large range of frequencies ( $0.001$  Hz  $< f < 0.05$  Hz). In this frequency range, as in TVF [3], we found that  $\alpha = \beta$  and  $\alpha = \beta = \sqrt{\pi f / D}$ . These two results are characteristic of a diffusion equation for the phase  $\Phi$  of the pattern with a diffusion constant  $D$ :

$$\frac{\partial \Phi}{\partial t} = D \frac{\partial^2 \Phi}{\partial x^2}. \quad (1)$$

Furthermore, this result shows that the phase diffusion

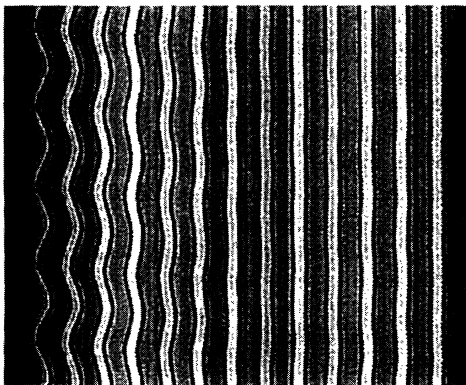


FIG. 3. Spatiotemporal representation of the position of the oil walls when the left boundary is forced to oscillate ( $f = 0.01$  Hz,  $Z_0 \approx 0.4\lambda$ ,  $L = 131$  mm,  $k = 0.64$  mm $^{-1}$ , and  $\epsilon = 0.16$ ). 500 s elapse from top to bottom. We found  $D = 18 \pm 2$  mm $^2$ /s, which is of the order of the oil viscosity.

dynamics is a pertinent description for the relaxation of perturbations imposed to the system, even quite far from the instability threshold where the cells are deep and have a highly nonlinear shape.

We then measured the evolution of the diffusion coefficient  $D$  at fixed wave number  $k$  when changing the  $\epsilon$  value [Fig. 4(a)]. When  $\epsilon$  is slowly decreased toward  $\epsilon_{min}(k)$ ,  $D$  decreases. This is in agreement with a classical Eckhaus instability at  $\epsilon_{min}(k)$  [2,3]. On the contrary, near  $\epsilon_{max}(k)$ ,  $D$  increases very abruptly, which corresponds to a more rigid pattern. By changing the frequency, we have verified that the phase still follows a diffusive equation near  $\epsilon_{max}(k)$ . Divergence of  $D$  was always observed, for the accessible range  $0.5 < \epsilon_{max}(k) < 2$ . The same general results were also observed for other values of  $L$  and  $k$ . This asymmetry between the low and high  $\epsilon$  limits is in agreement with the asymmetry of wavelength adjustment processes observed in DVF with open boundaries [10]. With these boundaries, the transients following a negative jump in  $\epsilon$  correspond to one cell shrinking and disappearing locally as in a classical Eckhaus scenario [12]. After a positive velocity jump the transients are characterized by a propagative localized state of broken

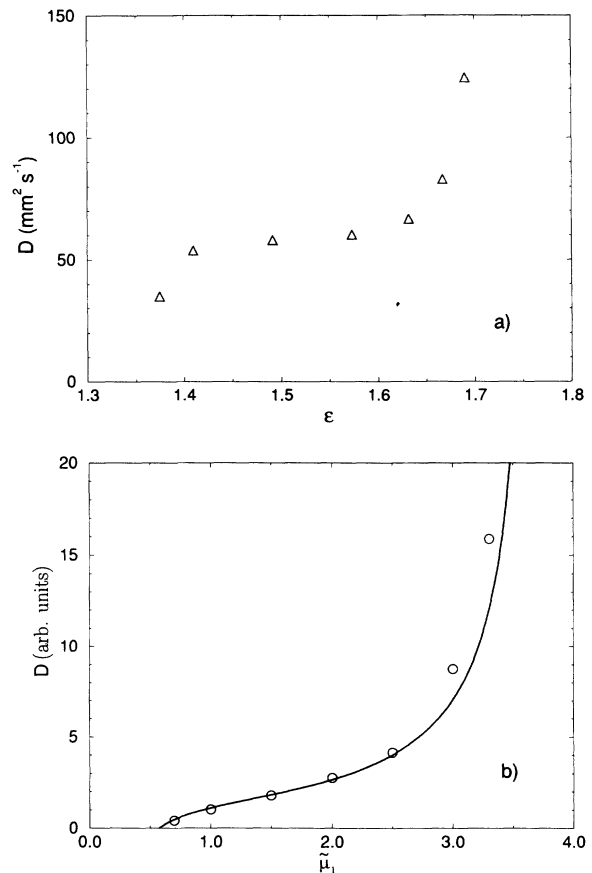


FIG. 4. Evolution of the phase diffusion coefficient  $D$  at fixed wave number  $k$ . (a) Experimental data ( $\Delta$ ) as a function of  $\epsilon$  for  $k = 1.54$  mm $^{-1}$ . (b) As a function of  $\bar{\mu}_1$ , calculated analytically (solid line) and numerically ( $\circ$ ). The chosen parameter values are  $\gamma = 1$ ,  $a_1 = 2$ ,  $\bar{\mu}_2 = -1$ ,  $c_1 = c_2 = 1$ ,  $d_1 = d_2 = 0.4$ , and  $k = 2\pi/20$ .

parity, which finally leads to the nucleation of a new cell. Such localized states were explained through a  $k$ - $2k$  mode interaction [7,8]. It has been pointed out that the  $k$ - $2k$  interaction is also important in the case of Taylor vortex flow [13].

We then tried to reproduce analytically the evolution of  $D$  near a parity-breaking bifurcation. In the vicinity of the codimension two point, where both the  $k$  and  $2k$  mode go unstable, we can describe the system in terms of two coupled amplitude equations. After the appropriate rescalings, these can be written as

$$\begin{aligned} \dot{A}_1 = & \tilde{\mu}_1 A_1 - \gamma A_1^* A_2 - a_1 |A_1|^2 A_1 - b_1 |A_2|^2 A_1 \\ & + c_1 \frac{\partial^2 A_1}{\partial x^2} + id_1 \frac{\partial A_1}{\partial x}, \end{aligned} \quad (2)$$

$$\begin{aligned} \dot{A}_2 = & \tilde{\mu}_2 A_2 + \gamma A_1^2 - a_2 |A_2|^2 A_2 - b_2 |A_1|^2 A_2 \\ & + c_2 \frac{\partial^2 A_2}{\partial x^2} + id_2 \frac{\partial A_2}{\partial x}, \end{aligned}$$

where the coefficients are all real. The last two terms, containing the partial derivative in space, are due to the curved nature of the marginal stability curve. The amplitude equations are derived from an expansion around the codimension two point while the experiments are performed away from this point. However, we will show below that, if we use these equations away from the codimension two point, they exhibit very similar behavior for the diffusion coefficient [14].

These equations have been studied previously in the analysis of the directional solidification of liquid crystals [15]. To simplify the algebraic complexity of the stability analysis that follows, we choose to present in this paper the case  $a_2 = b_1 = b_2 = 0$ . The essential physics, i.e., the existence of a mixed mode and a traveling mode, is still present for this particular choice of parameters and we have verified that the following results also hold in the general case.

It can be shown that the equations allow a mixed mode, i.e., where both the  $k$  and  $2k$  are present, and a traveling mode, i.e., a mode with a nonzero transversal velocity [16]. If we write  $A_1 = \rho e^{i\theta} e^{ikx}$  and  $A_2 = \sigma e^{i\phi} e^{2ikx}$  we can check that for the mixed mode (MM) we have

$$\rho^2 = \frac{\mu_1(k)\mu_2(k)}{\mu_2(k)a_1 - \gamma^2}, \quad \sigma = \frac{-\gamma\rho^2}{\mu_2(k)}, \quad (3)$$

while for the traveling mode (TW) we have

$$\rho^2 = 2\sigma^2 = \frac{2\mu_1(k) + \mu_2(k)}{2a_1}, \quad \cos(\chi) = \frac{\mu_2(k)}{2\gamma\sigma}, \quad (4)$$

where  $\chi = 2\theta - \phi$ ,  $\mu_1(k) = \tilde{\mu}_1 - c_1 k^2 - d_1 k$ , and  $\mu_2(k) = \tilde{\mu}_2 - 4c_2 k^2 - 2d_2 k$ . The TW exists if  $|\cos(\chi)| \leq 1$  and thus if the following parameter,  $C$ , is positive:

$$C = \mu_1(k) - \frac{a_1 \mu_2^2(k)}{2\gamma^2} + \frac{\mu_2(k)}{2}. \quad (5)$$

The TW bifurcates off the MM branch on the line where  $C$  becomes zero.

To investigate the stability of the MM against a variation of the wavelength of the underlying pattern, we replace the base solution by

$$A_1 = \rho (1 + \eta_q e^{iqx+st} + \eta_{-q} e^{-iqx+st}) e^{ikx} e^{i\theta}, \quad (6)$$

$$A_2 = \sigma (1 + \zeta_q e^{iqx+st} + \zeta_{-q} e^{-iqx+st}) e^{2ikx} e^{i\phi}.$$

Substituting the above expressions in Eq. (2), and linearizing in  $\eta_{\pm q}$  and  $\zeta_{\pm q}$  we obtain a  $4 \times 4$  matrix and its eigenvalues are the growth rates of the perturbation. The resulting characteristic equation does not contain odd powers of  $q$ . Therefore, to find the dispersion relation, and thus the diffusion constant  $D$ , we substitute  $s = s_0 + s_1 q^2 + \dots$  into the characteristic equation and solve order by order. At order 0 in  $q$ , we get four roots for  $s_0$ , one which is equal to zero and three which are negative. For the most dangerous mode, the one for which  $s_0 = 0$ , we get a dispersion relation of the form

$$s = -Dq^2 = \frac{F}{C}q^2, \quad (7)$$

where  $F$  is a complicated expression and  $C$  is defined in Eq. (5) above, and becomes zero at the onset of the TW. In other words, if we start in the MM state and approach the line which marks the onset of the TW, the diffusion constant  $D$  will *diverge*. We can also check that, for a large range of parameters,  $F$  is positive so that  $D$  diverges to  $+\infty$ . Furthermore, by solving  $D$  as a function of  $\tilde{\mu}_1$  we have verified that  $D$  goes through zero if one decreases  $\tilde{\mu}_1$ , which corresponds to an ordinary Eckhaus instability. A typical behavior of  $D$  as a function of  $\tilde{\mu}_1$  is plotted in Fig. 4(b). The qualitative behavior is identical to the one we have observed in the experiment. Note that this divergence is present for all parameter values.

To complete our analysis of the system, we have simulated the amplitude equations [Eq. (2)]. We have used a simple finite difference scheme in space and a fourth order Runge-Kutta in time. We took 20 wavelengths in our computational box, which had reflective boundary conditions. To mimic the moving boundary in the experiment, we have varied the phase of  $A_1$  and  $A_2$  at one of the boundaries sinusoidally with a fixed frequency and amplitude. Next, we determined  $D$  from the exponential spatial decay of the amplitude of the oscillations for each cell, as in the experiment. We see in Fig. 4(b) that the numerical results follow the analytical results closely.

In conclusion, we have presented a measurement of a phase diffusive constant  $D$  in a directional viscous fingering experiment and have reported the evolution of  $D$  when the pattern is compressed or stretched compared to its natural wavelength. In the case of compression,  $D$  decreases as expected when reaching an Eckhaus instability. In the case of stretching,  $D$  increases strongly. This is ascribed to the proximity of a parity-breaking instability and confirmed by the analytical and numerical study of coupled amplitude equations. The strong increase of the phase diffusion constant is a general result that should be observed in other systems exhibiting a parity-breaking bifurcation.

We thank Hermann Riecke for suggesting the possible link between an increase of the diffusion coefficient and a parity-breaking instability and for a fruitful discussion. The Laboratoire de Physique Statistique is "associé au CNRS et aux Universités Paris 6 et Paris 7."

- [1] Y. Pomeau and P. Manneville, *J. Phys. Lett. (Paris)* **40**, L609 (1979).
- [2] J.E. Wesfreid and V. Croquette, *Phys. Rev. Lett.* **45**, 634 (1980).
- [3] M. Wu and C.D. Andereck, *Phys. Fluids A* **4**, 2432 (1992).
- [4] W. Eckhaus, *Studies in Nonlinear Stability Theory* (Springer, New York, 1965).
- [5] K. Brattkus and C. Misbah, *Phys. Rev. Lett.* **64**, 1935 (1990).
- [6] H. Riecke and H.G. Paap, *Phys. Rev. A* **33**, 547 (1992).
- [7] C.A. Jones and M.R.E. Proctor, *Physics Lett. A* **121**, 224 (1987); M.R.E. Proctor and C.A. Jones, *J. Fluid Mech.* **188**, 301 (1988).
- [8] P. Couillet, R.E. Goldstein, and G.H. Gunaratne, *Phys. Rev. Lett.* **63**, 1954 (1989); S. Fauve, S. Douady, and O. Thual, *J. Phys. (France) II* **1**, 311 (1991).
- [9] J. Bechhoefer, A. Simon, A. Libchaber, and P. Oswald, *Phys. Rev. A* **40**, 2042 (1989); G. Faivre, S. de Cheveigné, C. Guthmann, and P. Kurowski, *Europhys. Lett.* **9**, 779 (1989); M. Rabaud, S. Michalland, and Y. Couder, *Phys. Rev. Lett.* **64**, 184 (1990); L. Limat, P. Jenffer, B. Dagens, E. Touron, M. Fermigier, and J.E. Wesfreid, *Physica D* **61**, 166 (1992); R.J. Wiener and D.F. McAlister, *Phys. Rev. Lett.* **69**, 2915 (1992); H.Z. Cummins, L. Fourtune, and M. Rabaud, *Phys. Rev. E* **47**, 1727 (1993); L. Pan and J.R. de Bruyn, *Phys. Rev. Lett.* **70**, 1791 (1993); I. Mutabazi and C.D. Andereck, *ibid.* **70**, 1429 (1993).
- [10] M. Rabaud, Y. Couder, and S. Michalland, *Eur. J. Mech. B* **10**, 253 (1991).
- [11] A similar change in wavelength selection has been demonstrated in TVF with rigid boundaries instead of smooth boundaries, i.e., ramps [G. Ahlers, D.S. Cannell, M.A. Dominguez-Lerma, and R. Heinrichs, *Physica D* **23**, 202 (1986); M. Lücke and D. Roth, *Z. Phys. B* **78**, 147 (1990)].
- [12] M. Lowe and J.P. Gollub, *Phys. Rev. Lett.* **55**, 2575 (1985).
- [13] H. Riecke and H.-G. Paap, *Phys. Rev. A* **45**, 8605 (1986); M.A. Dominguez-Lerma, D.S. Cannell, and G. Ahlers, *ibid.* **34**, 4956 (1986).
- [14] One can perform a similar analysis near the parity-breaking bifurcation on the basis of the amplitude equations describing the asymmetrical part of the pattern (Couillet *et al.* [8]). One can find again that the diffusion constant increases strongly as one approaches the parity-breaking bifurcation [H. Riecke (private communication)].
- [15] W.-J. Rappel and H. Riecke, *Phys. Rev. A* **45**, 846 (1992).
- [16] Note that the traveling waves are only present if we choose opposite signs for the coupling terms in Eq. (2).

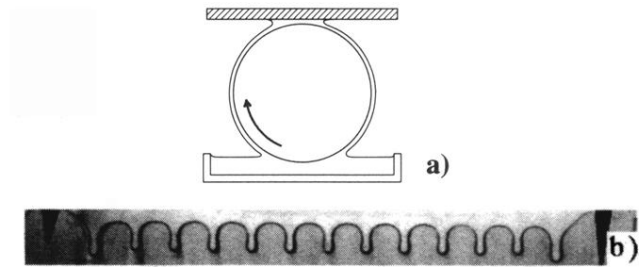


FIG. 1. (a) Sketch of the experimental setup. The rotating cylinder (radius 48 mm and length 236 mm) is partially immersed in a silicon oil bath (viscosity of  $\nu = 20 \text{ mm}^2/\text{s}$  at  $25^\circ\text{C}$ ), thermostated at  $25 \pm 0.1^\circ\text{C}$ . The coating film fills the small gap ( $b = 0.22 \pm 0.02 \text{ mm}$ ) between the upper glass plate and the cylinder, (b) picture of the unstable meniscus, constrained by two Mylar triangles located inside the gap with a spacing of  $L = 57 \text{ mm}$  (dimensionless cylinder velocity  $\epsilon = 1.72$ ).

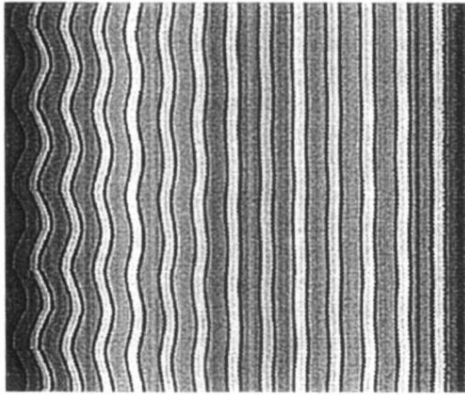


FIG. 3. Spatiotemporal representation of the position of the oil walls when the left boundary is forced to oscillate ( $f = 0.01$  Hz,  $Z_0 \approx 0.4\lambda$ ,  $L = 131$  mm,  $k = 0.64$  mm $^{-1}$ , and  $\epsilon = 0.16$ ). 500 s elapse from top to bottom. We found  $D = 18 \pm 2$  mm $^2$ /s, which is of the order of the oil viscosity.